Hydrophilic–Hydrophobic Patterned Molecularly Imprinted Photonic Crystal Sensors for High-Sensitive Colorimetric Detection of Tetracycline

Jue Hou, Huacheng Zhang, Qiang Yang, Mingzhu Li, Lei Jiang, and Yanlin Song**

Colorimetric sensors have attracted much attention because they do not need expensive or sophisticated instruments and they have been widely used in portable and rapid analysis especially for point-of-care testing.[1] Responsive photonic crystals (PCs) are promising materials for colorimetric detection owning to their vivid colors,[2] and they have been widely used in detection of molecules,[3] ions,[4] gas,[5] humidity,[6] electric field,[7] magnetic field,[8] and so on.[9] Combined with the molecularly imprinted polymer (MIP), the PC assay has become the most successful field of PCs application and realized selective and sensitive detection of small molecules[10] and proteins.[11] Although lots of MIP–PC colorimetric sensors have been achieved during the past decades, the design of structurally simple yet efficient devices for improving the sensitivity of MIP–PC detection still remains as a challenging task. Recently, enrichment process induced by wettability difference attracts widely attention because it provides an efficient strategy to improve the sensitivity of SERS[12] and fluorescent[13] analysis by enriching the targets from highly diluted solution to the sensitive area. Hydrophilic–hydrophobic pattern is a simple platform with wettability difference and it is the promising platform to realize enrichment process in practical application.

Here, we combined the MIP–PC colorimetric sensor with the enrichment process and fabricated a high-sensitive colorimetric sensor with hydrophilic–hydrophobic pattern for the first time to improve the sensitivity of tetracycline (TC) detection, which is of practical application in food testing and eco-pollution determination. This MIP–PC colorimetric sensor can realize larger than 200 nm colorimetric transition from cyan to red which is clearly recognized by naked eye. Besides, by changing the diameter of the detection area (MIP–PC dot) from 1.35 to 2.79 mm, the detection range of this sensor can vary from 10×10^{-9}–60×10^{-9} M to 10×10^{-9}–150×10^{-9} M. The limit of detection is down to 2×10^{-9} M by enriching a 10 μL droplet to a MIP–PC dot with diameter of 1.35 mm. This result is one order of magnitude lower than that of traditional MIP–PC film.[14] Moreover, the relationship between the size of detection area and the detection range was systematically investigated, and it has been concluded as a fan-shaped standard color card. This conclusion is of great importance for designing the sensors with suitable size of detection area and detection range in practical applications.

Figure 1a illustrates the fabrication process of the hydrophilic–hydrophobic patterned MIP–PC sensor. The MIP–PC dot was prepared by filling the precursor solution contained template TC molecule in the space of opal PC dot assembled by monodispersed colloidal spheres[15] on hydrophobic polydimethylsiloxane (PDMS) (Figure 1a i,ii). After the polymerization process, the template TC molecules and the colloidal spheres were removed and the MIP–PC sensor with hydrophilic MIP–PC dot and hydrophobic substrate was obtained (Figure 1a iii and see the Experimental Section). The PC sensor shown in Figure 1b comprises a series of opal PC dots on a hydrophobic PDMS substrate. It is worth mentioning that the purple PC dot was selected to be fabricated the MIP–PC dot in following experiment because it could be prepared as a cyan MIP–PC dot to provide much broader colorimetric transition range (from cyan to red) in visible light (Figures S1 and S2, Supporting Information). After fabrication process, the MIP–PC sensor with hydrophilic MIP–PC dots (CA = 10° ± 2.8°, Figure 1c) and hydrophobic substrate (CA = 115° ± 3.1°, Figure 1d) was obtained. The wettability difference between the MIP–PC dot and substrate can drive the analysts in the highly diluted solution to be enriched to the hydrophilic MIP–PC dot.

Former research has clearly proven the functional monomer acrylic acid (AA) in the polymerized MIP and the template TC molecule can form hydrogen bond, which proves the selective recognized structure for TC after removing the template TC molecule.[14] When a droplet of TC solution was dripped on the MIP–PC sensor, as the water evaporation, the

Dr. J. Hou, Dr. Q. Yang, Dr. M. Li,
Prof. L. Jiang, Prof. Y. Song
Beijing National Laboratory for
Molecular Sciences (BNLMS)
Key Laboratory of Green Printing
Key Laboratory of Organic Solids
Institute of Chemistry
Chinese Academy of Sciences
Beijing 100190, P.R. China
E-mail: mingzhu@iccas.ac.cn; ylsong@iccas.ac.cn
Dr. H. Zhang
Laboratory of Bio-inspired Smart Interface Science
Technical Institute of Physics and Chemistry
Chinese Academy of Sciences
Beijing 100190, P.R. China

DOI: 10.1002/smll.201403640

www.MaterialsViews.com

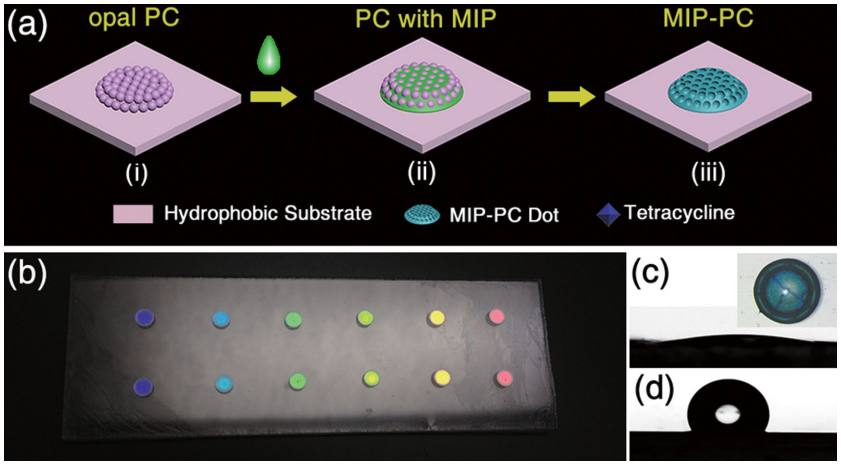

Figure 1. a) Scheme of the fabrication processes of the MIP–PC dot on hydrophobic substrate. b) Photography image of the PC sensor with different colors of PC dots. Contact angles of the MIP–PC dot c) (CA = 10° ± 2.8°) and PDMS substrate d) (CA = 115° ± 3.1°). (Inset) The microscope image of the MIP–PC dot in cyan color.

TC molecules in the droplet were enriched to the hydrophilic MIP–PC dot by wettability difference and selectively recognized by the MIP by forming hydrogen bond (**Figure 2**a). The spectra of MIP–PC dot during the enrichment gradually shifts (Figure 2b), so a suitable time to measure the spectra with the largest peak shift need to be found. A 10 µL droplet of 0.1×10^{-6} M TC was dripped on a MIP–PC dot with diameter of 1.35 mm. As the droplet evaporation, more and more TC molecules were enriched to the hydrophilic MIP–PC dot and recognized by the MIP. The peak position of the MIP–PC dot shifted from cyan to red in the first 10 min. When the droplet shrunk to the MIP-PC dot entirely, the red shift reached the maximum. After that, the MIP–PC dot became dried and the MIP structure shrunk, so the peak position shifted to blue gradually (Figure S3, Supporting Information). So in the following experiments, 10 min after a 10 µL droplet dripped on the MIP–PC dot is an optimized experimental parameter for measuring the spectrum in quantitative detection.

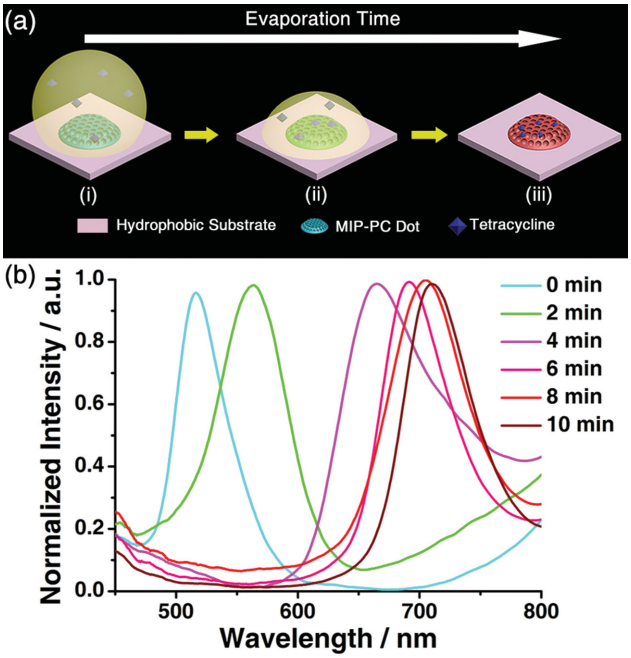

Figure 2. a) Schematic representation of the enrichment processes of TC molecules from highly diluted solution onto the MIP–PC dot for high-sensitive detection. As the water evaporation, the TC molecules are enriched to the MIP–PC dot to be selectively captured by the imprinted polymer and the color of the MIP–PC dot shifts to red. b) The spectra of the MIP–PC dot after dripping the TC solution, which illustrates the enrichment process of the TC molecules from the highly diluted solution to the MIP–PC dot.

The peak shift increases as the increasing of TC concentration. A series of 10 µL droplets with different TC concentrations (from 0×10^{-9} to 60×10^{-9} M) was dripped on the MIP–PC dots with diameter of 1.35 mm. As shown in **Figure 3**a, the color of the MIP–PC dot shifted from cyan to dark red as the concentration increasing. The peak position shift at corresponding TC concentration shifted from 504 nm (0×10^{-9} M) to 712 nm (60×10^{-9} M) (Figure 3b). The largest colorimetric transition range can reach 208 nm which can be clearly recognized by naked eye for qualitative or semiquantitative rapid detection. The peak position shift ($\Delta\lambda$) shows good linear relationship with the TC concentration (c) at 0×10^{-9}–60×10^{-9} M (Figure 3c), and the regression equation is $\Delta\lambda = 3.68\ c - 6.57$ with a correlation coefficient $r = 0.9962$. So this method could realize quantitative detection with the help of spectrometer and the limit of detection is down to 2×10^{-9} M.

The size of MIP–PC dot is a significant factor of this detection system because it influences the degree of solute enrichment. Here we fabricated a series of MIP–PC dot with different diameters and systematically researched the influence of the size of MIP–PC dot. 10 µL TC solution droplets with different volumes were dripped on the MIP–PC dots with diameters of 1.35, 1.92, 2.12, 2.41, and 2.79 mm, respectively (Table S1, Supporting Information). The relationships between the TC concentration (c) and the peak position shift ($\Delta\lambda$) at varied diameters of MIP–PC dots (d) are shown in **Figure 4**a. The results of each MIP–PC dot can be separated as two procedures: increasing procedure and saturation procedure. In the increasing procedure, $\Delta\lambda$ increases as the c increasing and shows good linear relationship. The linear fittings are very steep for the dots with diameter of 1.35 and 1.92 mm. The regression equations of the peak position shifts are $\Delta\lambda_1 = 3.68\ c - 6.57$ ($d_1 = 1.35$ mm, $r_1 = 0.9962$) and $\Delta\lambda_2 = 3.31\ c - 5.78$ ($d_2 = 1.92$ mm, $r_2 = 0.9946$). And the slopes are much gentler for the dots with diameters of 2.12, 2.41, and 2.79 mm. The corresponding regression equations are $\Delta\lambda_3 = 2.67\ c - 4.02$ ($d_3 = 2.12$ mm, $r_3 = 0.9983$), $\Delta\lambda_4 = 2.06\ c - 6.58$ ($d_4 = 2.41$ mm, $r_4 = 0.9977$), and $\Delta\lambda_5 = 1.56\ c - 11.64$ ($d_5 = 2.79$ mm, $r_5 = 0.9905$), respectively. The slopes of these fitting lines decreasing as the increasing diameters of the MIP–PC dots represent the degree of enrichment and the sensitivity of detection decrease. The linear ranges

DOI: 10.1002/smll.201403640

small NANO MICRO

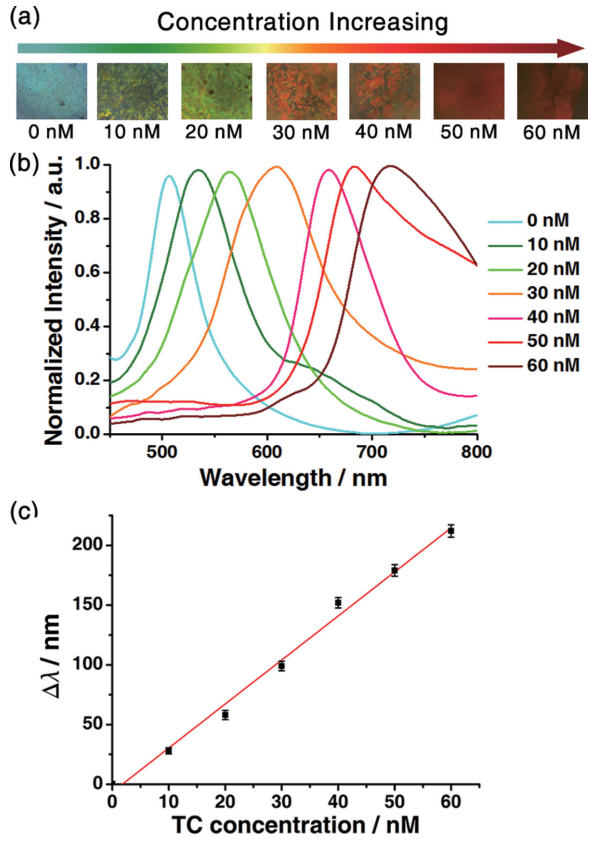

Figure 3. a) The colorimetric transition of the MIP–PC dot as the concentration increasing. The spectra b) and the peak position shift c) of 10 μL droplets with different concentrations dried on MIP–PC dots with diameter of 1.35 mm.

(or efficacious detection ranges) of the MIP–PC dots with diameters of 1.35, 1.92, 2.12, 2.41, and 2.79 mm are about 0×10^{-9}–60×10^{-9}, 0×10^{-9}–70×10^{-9}, 0×10^{-9}–80×10^{-9}, 0×10^{-9}–110×10^{-9}, and 0×10^{-9}–150×10^{-9} M, respectively. These results prove that the efficacious detection range increases as the increasing of the diameters of the MIP–PC dots. However, when the MIP–PC dots have been saturated, values of $\Delta\lambda$ reach the maximum (about 208 nm). The saturated concentrations of the MIP–PC dots with diameters of 1.35, 1.92, 2.12, 2.41, and 2.79 mm are 59×10^{-9}, 65×10^{-9}, 79×10^{-9}, 104×10^{-9}, and 141×10^{-9} M, respectively, calculated from the linear fitting results (Figure S4, Supporting Information). When the TC concentration reached to the saturated concentration, $\Delta\lambda$ did not continue to increase as the TC concentration increasing.

To further investigate the influence of the size of the MIP–PC dot on $\Delta\lambda$, the experimental data of 10×10^{-9} M TC droplets enriched on the MIP–PC dots with different sizes were shown in Figure 4b. $\Delta\lambda$ decreases with increasing the size of the MIP–PC dot (S) (S is calculated by $S = \pi d^2/4$) and the regression equation of the fitting line is $\Delta\lambda = -6.16\ S + 42.8$ ($r = 0.9840$). Similar results can be obtained by other TC concentrations. This result proves the sensitivity of the detection based on enrichment can be improved by decreasing the size of the hydrophilic detection area to increase the degree of enrichment.

The volume of the TC droplet is another important factor to influence the sensitivity of detection based on the enrichment process. TC droplets (10×10^{-9} M) with different volumes were dripped on the MIP–PC dots with same diameters (1.35 mm). As shown in Figure 4c, $\Delta\lambda$ increases with increasing the volume of droplet (V) and shows good linear relationship. The regression equation of the fitting line is $\Delta\lambda = 3.6\ V + 0.04$ ($r = 0.9990$). This result proves that dripping larger sample solutions is another way to improve the sensitivity of detection.

Furthermore, the detection result inspires a new strategy for design the sensors with different detection ranges by varying the size of the detection area in colorimetric detection based on enrichment process. The color corresponding to the TC concentration of each kind of MIP–PC dot was concluded in an intuitional figure (Figure 4d). The efficacious detection ranges of MIP–PC dots with varied diameters are presented by the height of the colorful bars. From that we can observe the influence of the size of MIP–PC dot in the detection range of colorimetric detection.

The experimental result can also be concluded as a fan-shaped standard color card (**Figure 5**) to show the relationship between the size of MIP–PC dot, tetracycline concentration and corresponding color. In this standard color card, all the dashes on each black curve illustrate the TC concentration of each kind of MIP–PC dot, and the color around this dash is the corresponding color of the experimental result. The maximum concentration of each curve illustrates the detection range of the corresponding MIP–PC dot. The users can choose the size of the MIP–PC dot based on the demanded detection range and compare the color of the MIP–PC dot after experiment with this standard color card to obtain half-quantitative TC concentration. The detection with varied detection ranges and sensitivity is demanded in practical applications. The concentration of TC in food is limited.[16] European Union (EU) has set the maximum residue limits (MRLs) for TC as 0.3 mg kg^{-1} in liver, 0.6 mg kg^{-1} in kidney, 0.2 mg kg^{-1} in egg, and 0.1 mg kg^{-1} (about 200×10^{-9} M) in milk or muscle tissues.[17] So a larger MIP–PC dot such as 2.79 mm can be used to obtain a broader detection range. While the maximum expected concentrations of wastewater treatment plant (WWTP) final effluents could not exceed 0.9 μg L^{-1} (about 2×10^{-9} M),[18] and the pesticide residues of TC in soil are often at μg/kg level.[19] So the user can choose the MIP–PC dot with diameter of 1.35 mm or even smaller to improve the sensitivity at low concentration. Besides, this strategy can be used in integrated sensor to achieve high-throughput detection with both multicomponents and multiranges.

In conclusion, we have fabricated a colorimetric sensor with high-sensitive TC detection based on a hydrophilic–hydrophobic patterned MIP–PC chip integrated with hydrophobic substrate and hydrophilic MIP–PC dots. The hydrophilic–hydrophobic patterned MIP–PC chip could enrich the target molecules from the diluted solution to the sensitive MIP–PC dot and realize naked-eye-recognized high-sensitive detection of the TC molecule down to 2×10^{-9} M. Moreover, the relationship between the size of the MIP–PC

DOI: 10.1002/smll.201403640

www.MaterialsViews.com

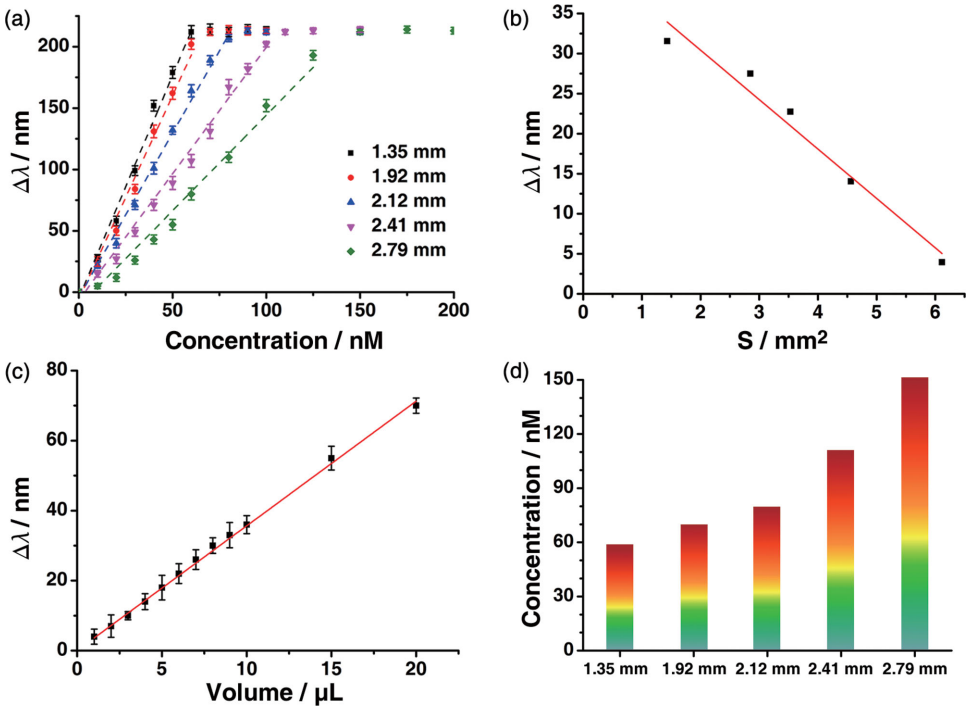

Figure 4. The influence of enrichment degree on the sensitivity of detection. a) The peak position shift of 10 μL TC solutions dripped on the MIP–PC dots with diameters of 1.35, 1.92, 2.12, 2.41, and 2.79 mm, respectively. The dashed lines are the linear fitting results. b) The relationship between the peak position shift in a) and the area of the PC dot at TC concentration of 10×10^{-9} M. The red line is the linear fitting result. c) The peak shift of TC solution (10×10^{-9} M) with different volumes dripped on the imprinted PC dot with diameter of 1.35 mm. The red line is the linear fitting result of the black dots. d) The color of the MIP–PC dot with different sizes under different TC concentrations. The height of the colorful bar presents the efficacious detection range of each kind of the MIP–PC dot.

dot, the sensitivity of detection, and the detection range of the target has also been systematically studied. The detection range of TC molecule increased from 0×10^{-9}–60×10^{-9} M to 0×10^{-9}–150×10^{-9} M as the diameter of the MIP–PC dot enlarged from 1.35 to 2.79 mm, while the sensitivity of TC detection decreased with increasing size of the MIP–PC dot. This work provides a good strategy to design high-sensitive colorimetric sensors for trace detection, as well as to well regulate the detection range by varying the size of sensitive area. This hydrophilic–hydrophobic patterned MIP–PC sensor has great potential applications in food safety, drug control, point-of-care testing, and eco-pollution determination.

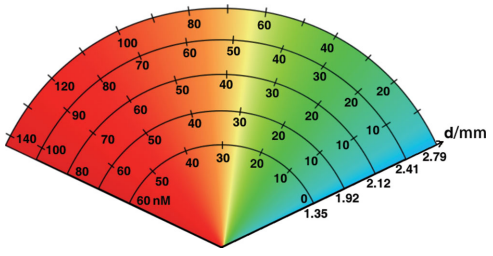

Figure 5. The fan-shaped standard color card to show the relationship between the diameter of the MIP–PC dot, tetracycline concentration, and corresponding color. In this color card, all the dashes on each black curve illustrate the TC concentration of corresponding MIP–PC dot. The maximum concentration of each curve illustrates the detection range of the corresponding MIP–PC dot.

Experimental Section

Preparation of PC Microchip with Opal Structure: PDMS (Sylgard 184 silicone elastomer kit, Dow) was mixed with the curing agent (10:1 w/w). Then the mixture was spin-coated on the glass slices (2000 r, 30 s). The slices were pre-cured at 60 °C for 15 min. The monodispersed latex spheres (P-(St-MMA-AA)) were synthesized by the emulsion polymerization method. Colloidal ink contained hydrophilic monodispersed latex spheres (5% wt%) in water and ethylene glycol (v:v, 1:3) was printed on a precured hydrophobic PDMS substrate. The droplet size varied from 1 to 5 μL. The printed microchips were dried in 60 °C, 60% RH, until the droplet completely dried. At last, the PC microchip was heated under 80 °C for 2 h to let the PDMS full-cured.

Preparation of MIP–PC Microchip with Inverse Opal Structure: 15 mL aqueous prepolymer solution with 7.5 g acrylamide (AAm, Acros), 3.42 g acrylic acid (AA, redistilled, Acros), 231 mg N,N′-methylene bisacrylamide (BIS, Alfa Aesar), 312 mg 2,2-diethoxyacetophenone (DEPO, Acros), and 10 mg tetracycline (TC, Alfa Aesar) was prepared to fabricate the TC MIP structure. The PC microchip with opal structure was dipped into the aqueous solution for 30 min. Then the microchip was pulled out and removed the extra solution by N_2 gas. After polymerization under the 100 W UV for 20 min, the microchip was first immersed in toluene to completely remove the colloidal crystal template, and then washed by 10% (v/v) acetic acid (Beijing Chemical Works) containing 10% (w/v) sodium dodecyl sulfate (SDS, Sigma-Aldrich) solution to remove the TC template in a bath oscillator at 70 °C for 2 h and rinsed thoroughly with deionized water until no further diffraction

small 2015,
DOI: 10.1002/smll.201403640

changes were observed, indicating full removal of TC from the MIP–PC dot. The MIP–PC microchip with inverse opal structure was obtained.

Measurement of the Reflectivity of the MIP–PC Dot: A 10 µL TC droplet was dipped on the imprinted PC dot. After 10 min, the droplet was dried and the solute (TC) was enriched on the MIP–PC dot. At this time, the wavelength of the MIP–PC dot could shift to red to the maximum. The spectrum was measured by spectrometer.

Characterization: Contact angles were captured by OCA20 instrument (DataPhysics, Germany) at 25 °C. Deionized water (MilliQ, 18.2 MΩ cm) was employed as the source for the CA measurement. The values reported were the average of five drops at different locations. The reflection spectra were collected by microscope (BX51, Olympus Co., Ltd) with an UV–vis spectrometer (NOVA, Ideaoptics Technology Ltd., China). SEM images of the PCs were obtained using a field-emission scanning electron microscope (JEOL-4800, Tokyo, Japan). The images of the PC dots were captured by stereo microscope (SteREO Discovery.V8, Zeiss, Germany) and microscope (BX51, Olympus Co., Ltd).

Supporting Information

Supporting Information is available from the Wiley Online Library or from the author.

Acknowledgements

This work was supported by the NSFC (Grant Nos. 51473173, 51173190, 21003132, 91127038, and 21121001), the 973 Program (Grant Nos. 2013CB933004, 2011CB932303, and 2011CB808400), Beijing Nova Program (Grant No. Z131103000413051), and the "Strategic Priority Research Program" of the Chinese Academy of Sciences (Grant No. XDA09020000).

[1] a) E. Tan, J. Wong, D. Nguyen, Y. Zhang, B. Erwin, L. K. Van Ness, S. M. Baker, D. J. Galas, A. Niemz, *Anal. Chem.* **2005**, *77*, 7984; b) C. D. Medley, J. E. Smith, Z. Tang, Y. Wu, S. Bamrungsap, W. Tan, *Anal. Chem.* **2008**, *80*, 1067; c) A. K. Ellerbee, S. T. Phillips, A. C. Siegel, K. A. Mirica, A. W. Martinez, P. Striehl, N. Jain, M. Prentiss, G. M. Whitesides, *Anal. Chem.* **2009**, *81*, 8447; d) J. I. Hong, B. Y. Chang, *Lab Chip* **2014**, *14*, 1725.

[2] a) Y. J. Zhao, X. W. Zhao, Z. Z. Gu, *Adv. Funct. Mater.* **2010**, *20*, 2970; b) J. Ge, Y. Yin, *Angew. Chem. Int. Ed.* **2011**, *50*, 1492; c) J. Wang, Y. Zhang, S. Wang, Y. Song, L. Jiang, *Acc. Chem. Res.* **2011**, *44*, 405; d) Y. Zhao, Z. Xie, H. Gu, C. Zhu, Z. Gu, *Chem. Soc. Rev.* **2012**, *41*, 3297; e) C. Fenzl, T. Hirsch, O. S. Wolfbeis, *Angew. Chem. Int. Ed.* **2014**, *53*, 3318; f) Y. Zhao, L. Shang, Y. Cheng, Z. Gu, *Acc. Chem. Res.* **2014**, *47*, 3632; g) H. Gu, Y. Zhao, Y. Cheng, Z. Xie, F. Rong, J. Li, B. Wang, D. Fu, Z. Gu, *Small* **2013**, *9*, 2266; h) Y. Zhao, Y. Cheng, L. Shang, J. Wang, Z. Xie, Z. Gu, *Small* **2015**, *11*, 151; i) Z. Xie, L. Li, P. Liu, F. Zheng, L. Guo, Y. Zhao, L. Jin, T. Li, Z. Gu, *Small* DOI: 10.1002/smll.201402071.

[3] a) J. H. Holtz, S. A. Asher, *Nature* **1997**, *389*, 829; b) S. A. Asher, V. L. Alexeev, A. V. Goponenko, A. C. Sharma, I. K. Lednev, C. S. Wilcox, D. N. Finegold, *J. Am. Chem. Soc.* **2003**, *125*, 3322; c) H. L. Li, J. X. Wang, L. M. Yang, Y. L. Song, *Adv. Funct. Mater.* **2008**, *18*, 3258.

[4] a) K. Lee, S. A. Asher, *J. Am. Chem. Soc.* **2000**, *122*, 9534; b) C. E. Reese, S. A. Asher, *Anal. Chem.* **2003**, *75*, 3915; c) X. Hu, J. Huang, W. Zhang, M. Li, C. Tao, G. Li, *Adv. Mater.* **2008**, *20*, 4074; d) X. Li, L. Peng, J. Cui, W. Li, C. Lin, D. Xu, T. Tian, G. Zhang, D. Zhang, G. Li, *Small* **2012**, *8*, 612.

[5] a) C. Liu, G. Gao, Y. Zhang, L. Wang, J. Wang, Y. Song, *Macromol. Rapid. Commun.* **2012**, *33*, 380; b) L. Bai, Z. Xie, W. Wang, C. Yuan, Y. Zhao, Z. Mu, Q. Zhong, Z. Gu, *ACS Nano* **2014**, *8*, 11094; c) Z. Xie, K. Cao, Y. Zhao, L. Bai, H. Gu, H. Xu, Z. Z. Gu, *Adv. Mater.* **2014**, *26*, 2413; d) C. Cui, Y. Liu, H. Xu, S. Li, W. Zhang, P. Cui, F. Huo, *Small* **2014**, *10*, 3672.

[6] a) E. T. Tian, J. X. Wang, Y. M. Zheng, Y. L. Song, L. Jiang, D. B. Zhu, *J. Mater. Chem.* **2008**, *18*, 1116; b) L. B. Wang, J. X. Wang, Y. Huang, M. J. Liu, M. X. Kuang, Y. F. Li, L. Jiang, Y. L. Song, *J. Mater. Chem.* **2012**, *22*, 21405.

[7] a) L. Xu, J. Wang, Y. Song, L. Jiang, *Chem. Mater.* **2008**, *20*, 3554; b) D. P. Puzzo, A. C. Arsenault, I. Manners, G. A. Ozin, *Angew. Chem., Int. Ed.* **2009**, *48*, 943.

[8] a) J. Ge, Y. Hu, Y. Yin, *Angew. Chem. Int. Ed.* **2007**, *46*, 7428; b) H. Kim, J. Ge, J. Kim, S. Choi, H. Lee, H. Lee, W. Park, Y. Yin, S. Kwon, *Nat. Photonics* **2009**, *3*, 534; c) Y. Hu, L. He, Y. Yin, *Angew. Chem. Int. Ed.* **2011**, *50*, 3747; d) L. He, M. Wang, J. Ge, Y. Yin, *Acc. Chem. Res.* **2012**, *45*, 1431.

[9] a) H. Fudouzi, Y. Xia, *Adv. Mater.* **2003**, *15*, 892; b) J. Ge, J. Goebl, L. He, Z. Lu, Y. Yin, *Adv. Mater.* **2009**, *21*, 4259.

[10] a) X. Hu, Q. An, G. Li, S. Tao, J. Liu, *Angew. Chem., Int. Ed.* **2006**, *45*, 8145; b) Z. Wu, X. Hu, C. Tao, Y. Li, J. Liu, C. Yang, D. Shen, G. Li, *J. Mater. Chem.* **2008**, *18*, 5452.

[11] a) X. B. Hu, G. T. Li, J. Huang, D. Zhang, Y. Qiu, *Adv. Mater.* **2007**, *19*, 4327; b) Y. J. Zhao, X. W. Zhao, J. Hu, J. Li, W. Y. Xu, Z. Z. Gu, *Angew. Chem. Int. Ed.* **2009**, *48*, 7350.

[12] a) F. De Angelis, F. Gentile, F. Mecarini, G. Das, M. Moretti, P. Candeloro, M. L. Coluccio, G. Cojoc, A. Accardo, C. Liberale, R. P. Zaccaria, G. Perozziello, L. Tirinato, A. Toma, G. Cuda, R. Cingolani, E. Di Fabrizio, *Nat. Photonics* **2011**, *5*, 682; b) F. Gentile, M. L. Coluccio, N. Coppede, F. Mecarini, G. Das, C. Liberale, L. Tirinato, M. Leoncini, G. Perozziello, P. Candeloro, F. De Angelis, E. Di Fabrizio, *ACS Appl. Mater. Interfaces* **2012**, *4*, 3213.

[13] J. Hou, H. Zhang, Q. Yang, M. Li, Y. Song, L. Jiang, *Angew. Chem. Int. Ed.* **2014**, *53*, 5791.

[14] L. Q. Wang, F. Y. Lin, L. P. Yu, *Analyst* **2012**, *137*, 3502.

[15] J. X. Wang, Y. Q. Wen, H. L. Ge, Z. W. Sun, Y. M. Zheng, Y. L. Song, L. Jiang, *Macromol. Chem. Phys.* **2006**, *207*, 596.

[16] a) R. J. McCracken, W. J. Blanchflower, S. A. Haggan, D. G. Kennedy, *Analyst* **1995**, *120*, 1763; b) J. R. Walsh, L. V. Walker, J. J. Webber, *J. Chromatogr. A* **1992**, *596*, 211.

[17] *Off. J. Eur. Communities* **1990**, *224*.

[18] X. S. Miao, F. Bishay, M. Chen, C. D. Metcalfe, *Environ. Sci. Technol.* **2004**, *38*, 3533.

[19] B. Suarez, B. Santos, B. M. Simonet, S. Cardenas, M. Valcarcel, *J. Chromatogr. A* **2007**, *1175*, 127.

Received: December 8, 2014
Revised: January 9, 2015
Published online: